

Research Article

Simulation and Experimental Verification of Intelligence MPPT Algorithms for Standalone Photovoltaic Systems

¹M. Muthuramalingam and ²P.S. Manoharan

¹P.T.R College of Engineering and Technology,

²Thiagarajar College of Engineering, Madurai, Tamilnadu, India

Abstract: This study presents compared with Fuzzy Logic Control (FLC) and Adaptive Neuro-Fuzzy Inference System (ANFIS) Maximum Power Point Tracking (MPPT) algorithms, in terms of parameters like tracking speed, power extraction, efficiency and harmonic analysis under various irradiation and cell temperature conditions of Photovoltaic (PV) system. The performance of a PV array are affected by temperature and solar irradiation, In fact, in this system, the experimental implementation and the MATLAB based simulations are In this topology, each Cascaded H-Bridge Inverter (CHBI) unit is connected to PV module through an Interleaved Soft Switching Boost Converter (ISSBC). It also offers another advantage such as lower ripple current and switching loss compared to the conventional boost converter. The results are evaluated by simulation and experimental implemented on a 150 W PV panel prototype with the microcontroller platform. The simulation and hardware results show that ANFIS algorithm is more efficient than the FLC algorithm.

Keywords: Cascade H-Bridge Inverter (CHBI), Interleaved Soft Switching Boost inverter (ISSBC), Maximum Power Point Tracking (MPPT), microcontroller, Photovoltaic (PV) system

INTRODUCTION

Photovoltaic energy has increased interest in electrical power applications, since it is considered as a fundamentally endless and generally available energy resource. However, the output power induced in the photovoltaic modules depends on solar irradiance and temperature of the solar cells. Therefore, to maximize the efficiency of the renewable energy system, it is compulsory to track the maximum power point of the PV array. This point is called the Maximum Power Point (MPP). The locus of this point has a nonlinear variation with solar irradiance (G) and the cell Temperature (T). Thus, in order to operate the PV array at its MPP, the PV system must include a Maximum Power Point Tracking (MPPT) controller (Gao *et al.*, 2013).

Many MPPT techniques have been reported in the literature such as perturb and observation, incremental conductance, (Hohm and Ropp, 2000; Eram and Chapman, 2007; Safari and Michele, 2011) artificial neural network, fuzzy logic based controller (Ben Salah and Ouali, 2011; Alajmi *et al.*, 2011; Kottas *et al.*, 2006; Salhi and El-Bachtri, 2011) ANFIS (Putri and Rifa, 2012; Mellit and Kalogeria, 2011) etc. In this study FLC and ANFIS MPPT algorithm being used to extract the maximum DC power from PV module. The generated DC power is converted into AC, in order to be used in a standalone system. In recent times,

multilevel inverter topologies have received more attention to the use in PV applications (Beser *et al.*, 2010). The output waveforms are much improved over conventional inverter. This leads to harmonics in the output voltage and current of the multilevel inverter (Leon *et al.*, 2013). To overcome the difficulties, in this study, single phase selective harmonic elimination ANN integrated modulation technique is proposed and verified.

METHODOLOGY

Stand alone PV system: The block diagram of the proposed topology for ISSBC and CHBMLI based stand-alone PV system is shown in Fig. 1, the inverter is fed from photovoltaic module through a DC-DC converter integrated with FLC and ANFIS MPPT algorithm. The output of the single phase SHE trained ANN unit has been applied to the CHBI to achieve a balanced output with improved power quality even under non-ideal condition of PV cell. To analyze and compare FLC and ANFIS MPPT algorithms for different conditions such as changing solar irradiation and cell temperature. The simulation results are validated experimentally in a hardware setup with the 16F877A microcontroller platform.

PV array modeling and simulation: The PV array used in the proposed system is 72 multi-crystalline

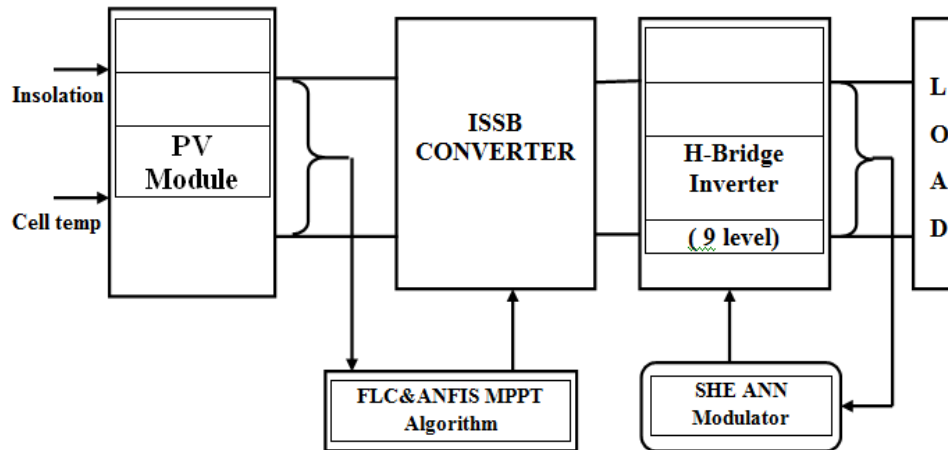


Fig. 1: General diagram of load connected photovoltaic system

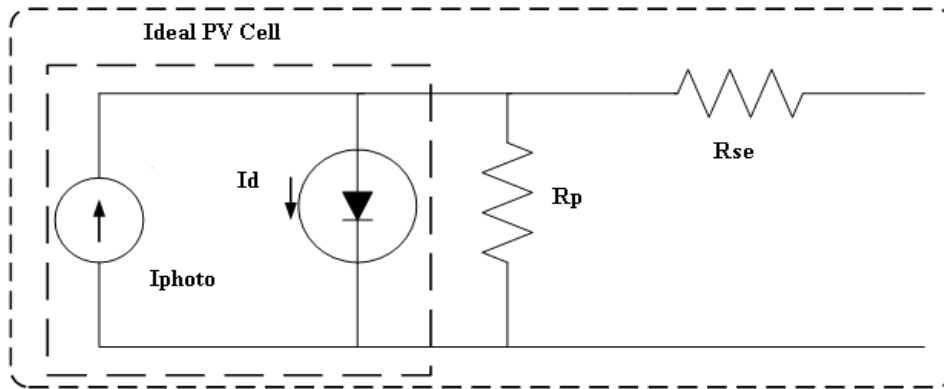


Fig. 2: Equivalent model of the PV panel

Table 1: PV module parameter

Parameter	
Maximum power (Pmax)	150 W
Voltage at Pmax (Vmp)	34.50 V
Current at Pmax (Imp)	4.35 A
Open-circuit voltage (Voc)	43.50 V
Short-circuit current (Isc)	4.75 A

silicon solar cells in series and able to provide 150 W of maximum power. In this model, a PV cell is represented by a current source in parallel with a diode and a series resistance as shown in Fig. 2. The basic current equation is given in Eq. (1):

$$I = I_{pv, cell} - I_{0, cell} \left[\exp \frac{qV}{akT} - 1 \right] \quad (1)$$

where, $I_{PV, Cell}$ is current generated by the incident light (directly proportional to sun irradiation), $I_{0, Cell}$ is leakage current of the diode, q is electron charge 1.6021×10^{-19} C, k is Boltzmann constant (1.38×10^{-23} J/K), T is Temperature of the PN junction and a is diode ideality constant. To develop embedded SIMULINK model based on current equation and

manufacturer's data sheet parameter of BP SX 150S model as shown in Table 1.

MPPT control algorithms: The MPPT algorithm is used for extracting the maximum power from the PV module and passes it on to the load. A converter serves the purpose of transferring maximum power from the solar PV module to the load. By changing the duty cycle the load impedance, as seen by the source, is varied and matched at the point of the peak power with the source so as to transfer the maximum power.

FLC MPPT controller: The FLC MPPT algorithm is used to ISSBC to compensate the output voltage of PV system to keep the voltage at the value which maximizes the output power. The fuzzy logic controller consists of three basic elements, namely fuzzification, rule base inference engine and defuzzification.

Fuzzification comprises the process of transforming numerical crisp inputs into linguistic variables based on the degree of membership to certain sets. The fuzzification variables are logical decision framed in inference engine block and deliver linguistic

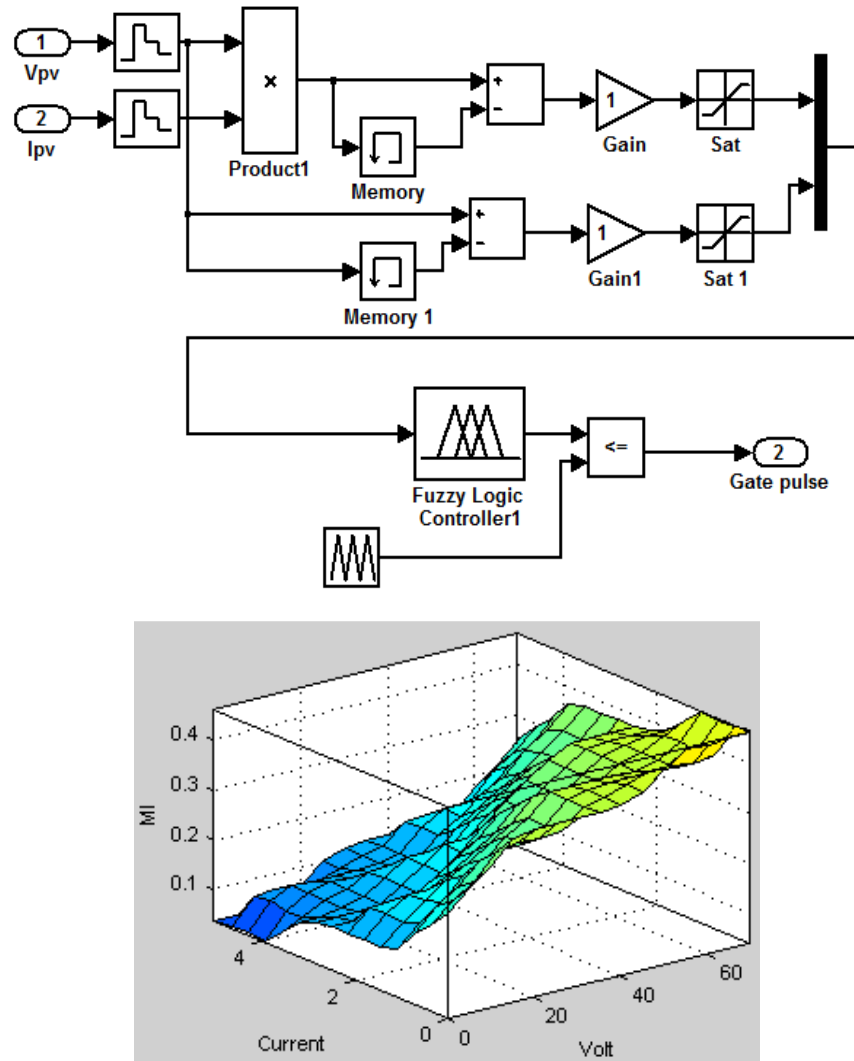


Fig. 3: FLC MPPT control system and FLC surface output

output. Defuzzifier is used to convert linguistic fuzzy sets to actual value. In this study the fuzzy inference rule is carried out by using Mamdani's method and the defuzzification use the centre of gravity to compute the output of this FLC which is the duty cycle. The SIMULINK controller and surface output shown in Fig. 3. The two FLC input variables are the error $E(k)$ and change of error $CE(k)$ at sampled times k defined in Eq. (2):

$$E(k) = \frac{P_{pv(k)} - P_{pv(k-1)}}{V_{pv(k)} - V_{pv(k-1)}} \quad (2)$$

$$CE(k) = E(k) - E(k-1) \quad (3)$$

where, $P(k)$ and $V(k)$ are the instant power and voltage of the photovoltaic system, respectively $E(k)$ is zero at the maximum power point of PV array. The input $E(k)$ shows if the operation point at the instant k is located on the left or on the right of the MPPT on the PV

Characteristic while the input $CE(k)$ expresses the moving direction of this point Eq. (3).

ANFIS MPPT algorithm: The ANFIS system is used to formulate the neural network architecture in the inference engine of a Fuzzy controller. The functional block diagram and structure of ANFIS is shown in Fig. 4. The structure comprises of three distinct layers namely input layer, hidden layer and output layer. The ANFIS controller implemented in this study is of the model described as above whose fuzzifier section comprises of the input signals error (e) and change in error signal (ce) whose membership functions are selected as Gaussian membership function. The defuzzifier of the ANFIS is the output function that is the modulation index (d).

The input membership functions are mapped to the output membership function by 49 rules through grid partitioning method using the FIS generator in MATLAB SIMULINK. The 2500 data sets to train

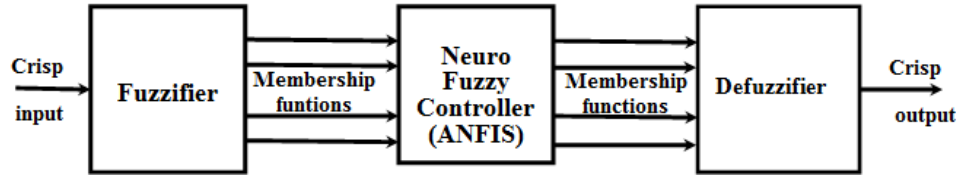


Fig. 4: ANFIS control system

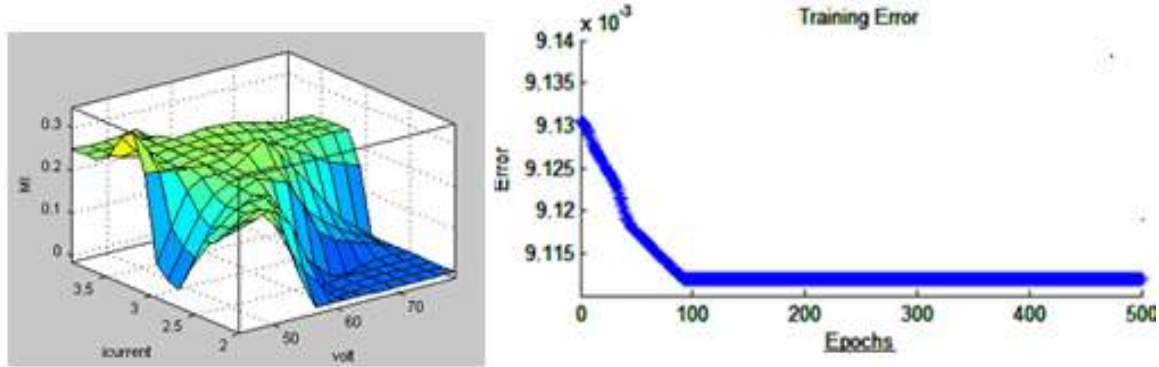


Fig. 5: ANFIS surface view and training error

ANFIS is obtained from workspace from the previous FLC MPPT algorithm model in which data's namely PV voltage and current and the corresponding modulation index (MI). The learning data trained through back propagation technique for 500 epochs for minimum error tolerance. The network training is performed repeatedly until the performance indexes $E_p = (V_{ref} - V_{pv})^2$ reduce below a specified value ideally to zero. In other words when $E_p \rightarrow 0$ leads to $(V_{ref} - V_{pv})^2 \rightarrow 0$, then the trained ANFIS connecting weights are adjusted in such a way that the estimated array voltage is identically equal to the MPP voltage. The trained surface rule phase view and training error shown in Fig. 5, the trained data set exports the simulation and observes the performance different weather condition.

Soft switching boost converter: It serves as a suitable interface for PV cells to convert low voltage, high current input into a high voltage low current output. The interleaved boost inverter consists of two single phase boost inverters that are connected in parallel and inverters operating 180° out of phase with 30 kHz switching frequency (Jung *et al.*, 2011). It is pointed out that in interleaved inverter mode 60 kHz effect is achieved by phase shifting of the two 30 kHz switching signals. Because the inductor ripple currents are out of phase, they cancel each other and the input-ripple current reduce to 12% of that of a conventional boost inverter. The best input-inductor-ripple-current cancellation occurs at 50% duty cycle.

Single phase CHB inverter: The cascaded multilevel inverter is composed of a number of H-bridge inverter units with separate DC source for each unit and can be connected in cascade to produce a near sinusoidal output voltage waveform. There are different switching strategies implemented for minimization and elimination of harmonics (Tsang and Chan, 2013; Ravi *et al.*, 2011). This fact leads to distortion in the output voltage waveform of the multilevel power inverter:

$$V_{ab}(wt) = \sum_{n=1,5,7,11,\dots}^{\infty} \left[\frac{4}{\pi n} (V_{pv1} \cos(n\alpha_1) + V_{pv2} \cos(n\alpha_2)) \right] \quad (4)$$

In this study selective harmonic elimination pulse with modulation technique is implemented to generate the switching duty cycle for CHB inverter. The Eq. (4) shows the contents of the output voltage at infinite frequencies, the module voltage $V_{pv1}-V_{pv2}$ are associated to their respective switching angle $\alpha_1-\alpha_2$. These trigonometric transcendental equations can be solved by GA and implemented to find the switching angle (offline) for a set of predetermined modulation indices to get the required fundamental output voltage in a nine level cascaded multi level inverter. The switching angles (α_1, α_2) lie in between 0 and $\pi/2$.

RESULTS AND DISCUSSION

Simulation results: The SIMULINK software validates the performance of the MPPT techniques under different operating conditions. The parameters are considered in the Standard Test Condition (STC): 1000 W/m^2 and cell temperature of 25°C . The simulation circuit diagram is shown in Fig. 6. The

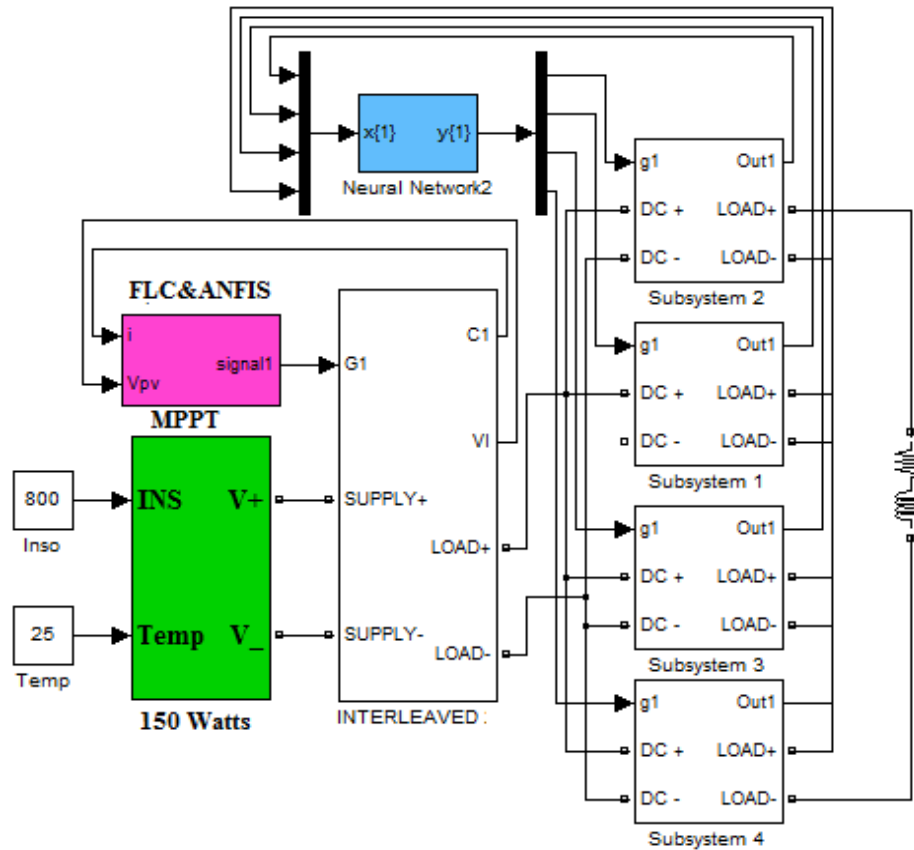


Fig. 6: Simulation system

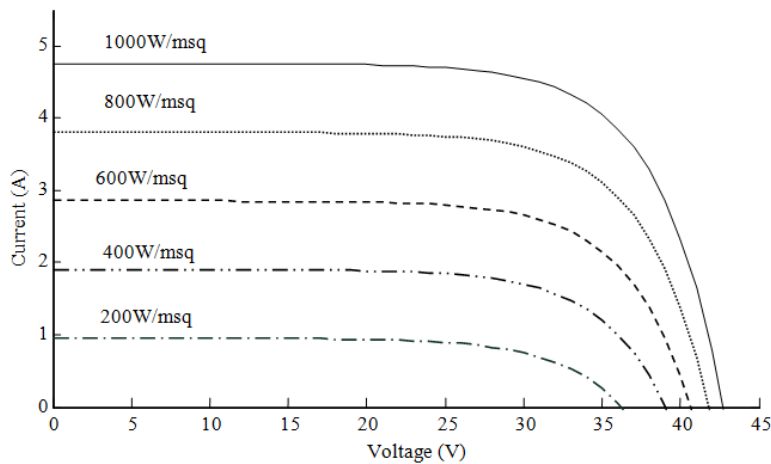


Fig. 7: I-V curve at 25°C

simulation validation of PV module and converter results of the I-V and P-V characteristics of PV module as a function of irradiation and temperature shown in Fig. 7 and 8. It can be observed quite similar to the PV module as per data sheet. In order to achieve the maximum power point of PV modules, FLC and ANFIS MPPT controller has been developed using MATLAB SIMULINK model. The simulation result is presented for the following different configurations:

- Converter alone:
 - Dynamic variation of irradiation
 - Dynamic variation of temperature
- Converter and Inverter constant irradiation and temperature

Simulations are carried out for the two techniques under dynamically changing solar irradiances at temperature of 25°C. Figure 9 shows output power of

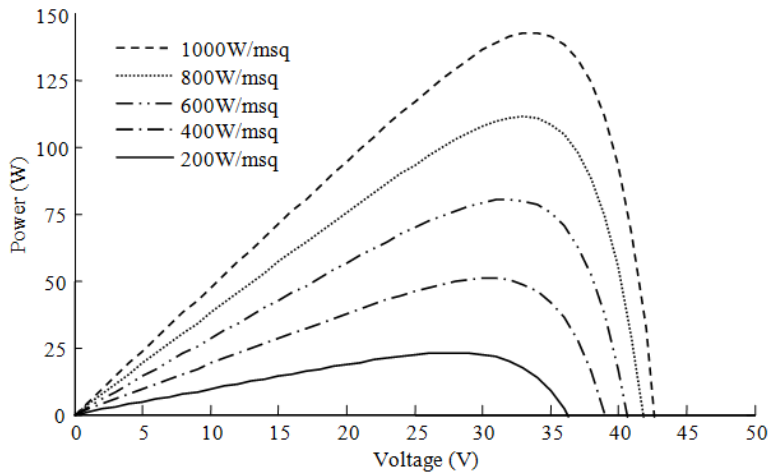


Fig. 8: P-V curve at 25°C

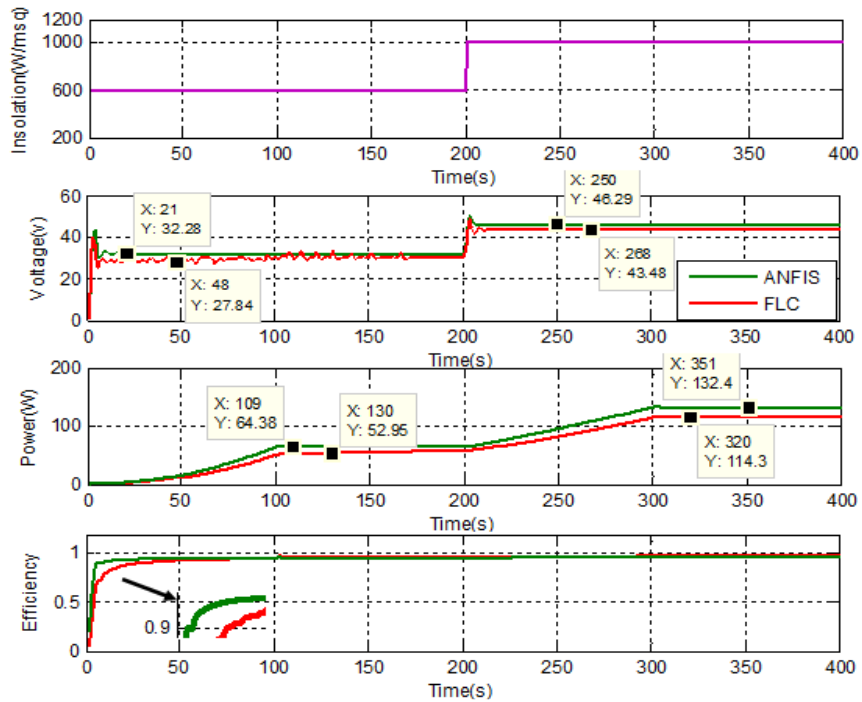


Fig. 9: Dynamic behavior insolation voltage, power and efficiency

Table 2: Dynamic behavior of irradiation

Insolation (W/m ²)	Temperature (°C)	FLC		ANFIS	
		Power (W)	Efficiency (%)	Power (W)	Efficiency (%)
600	25	52.95	97.5	64.38	98.75
1000	25	114.30	97.2	132.40	98.61

sudden changes in solar irradiation from 600 to 1000 W/m². In this analysis, the two techniques are able to extract the MPP, the detailed simulation result, voltage, power and corresponding efficiency tabulated in Table 2. Observed result, the ANFIS more power extracted and fast response to reach the new MPP, after solar irradiation changes compared to FLC also gives a fast steady state response with less oscillation.

Dynamic variation of the solar irradiation: Simulations are carried out for the two techniques under dynamically changing solar irradiances at temperature of 25°C. Figure 9 shows output power of sudden changes in solar irradiation from 600 to 1000 W/m². In this analysis, the two techniques are able to extract the MPP, the detailed simulation result, voltage, power and corresponding efficiency tabulated in Table 2.

Table 3: Dynamic behavior of temperature

Insolation (W/m ²)	Cell temperature (°C)	FLC		ANFIS	
		Power (W)	Response time (msec)	Power (W)	Response time (msec)
900	25	101.40	141	121.8	126
	50	94.49	350	109.3	150

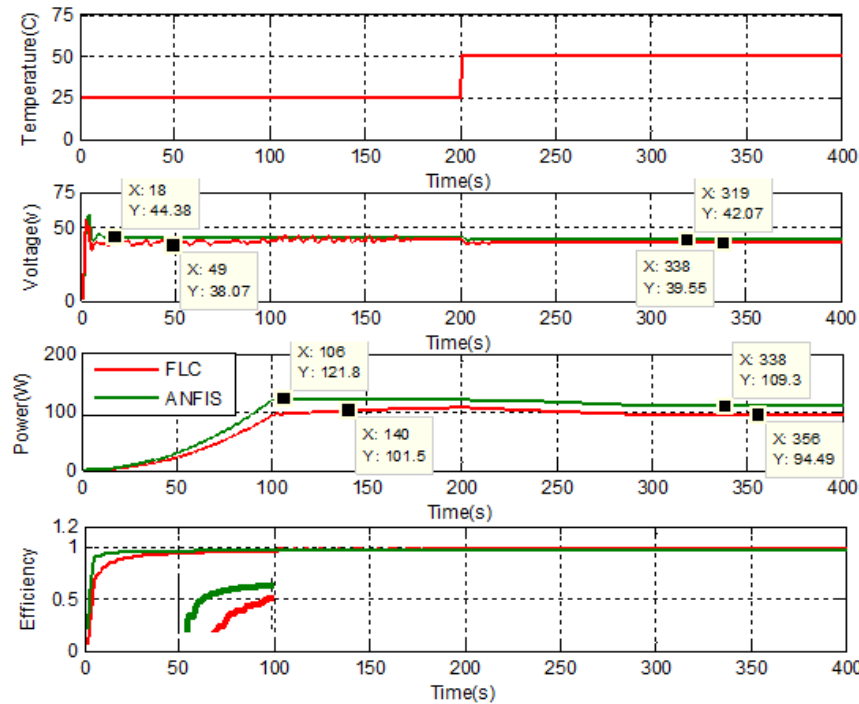


Fig. 10: Dynamic behavior cell temperature

Observed result, the ANFIS more power extracted and fast response to reach the new MPP, after solar irradiation changes compared to FLC also gives a fast steady state response with less oscillation.

Dynamic variation of cell temperature: This simulation is carried out to illustrate the performance of the MPPT methods under constant solar irradiation of 900 W/m² and changes in temperature from 25 to 50°C. The temperature has a slight effect on the cutoff circuit current. However, the open circuit voltage decays quickly as the temperature increases. Figure 10 shows the corresponding PV voltage. Power and efficiency, during slowly occurring as well as sudden changes in temperature, respectively, the FLC and ANFIS the maximum extracted power and response time tabulated in Table 3. When compared to ANFIS the FLC does not converge to the globally maximum power point. The ANFIS exhibits fast response and also converges to the globally maximum power point with slight fluctuations and highest PV output power in the change in dynamics of temperature.

Simulation with converter and inverter: Finally, in order to verify the performances of the FLC and ANFIS algorithm, the CHBI is connected to an RL load

(R = 100 ohm and L = 20 mH) using switching frequency of 30 kHz in the ISSBC. The PV array receives constant solar irradiation of 1000 W/m² cell temperature at 25°C.

The converter output voltage injected to the H-bridge inverter, the output of the stepped modulated inverter voltage, along with their harmonic spectrum (7.5 KHz) of the FLC and ANFIS algorithms are shown in Fig. 11 and 12, respectively. The Total Harmonic Distortion (THD) of the output voltage with the FLC model of control is 29.54% and with the ANFIS model they are 25.62%, respectively. It can be observed from the simulation results the percentage THD is less in ANFIS algorithm as compared to the FLC algorithm.

Experimental validation: The simulation results were verified experimentally in the using the appropriate hardware built around the PIC 16F877A microcontroller as shown in Fig. 13. The solar panels are not shown in photograph. The controller program is downloaded into microcontroller and generates gating signals to the ISSBC and CHBI. For the validation of maximum power point tracking control, the developed system is tested at 9.00 h, 13:15 and 16.15 h. The irradiation and temperature were measured as 350 W/m² 35.6°C 1050 W/m² 35°C and 625 W/m² 36°C,

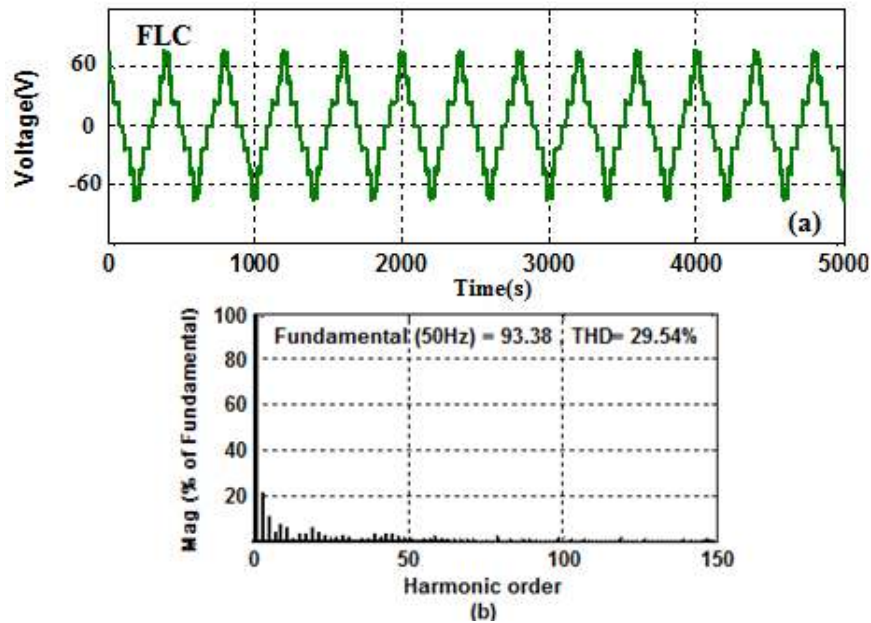


Fig. 11: Simulation of FLC MPPT (a) output voltage (b) harmonic spectrum

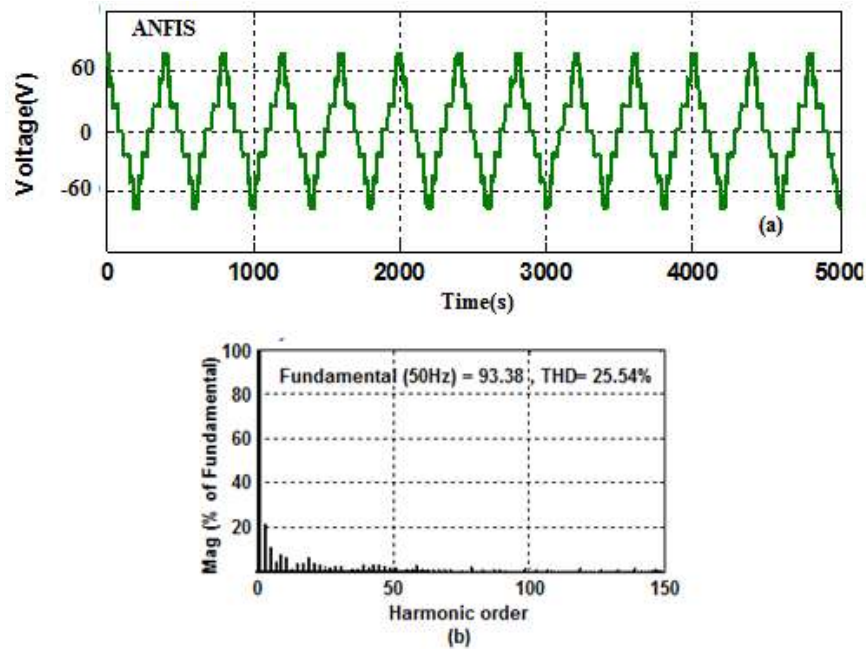


Fig. 12: Simulation of ANFIS MPPT (a) output voltage (b) harmonic spectrum

Table 4: Experimental pattern

Pattern	Insulation (W/m ²)	Temperature (°C)
Case 1	350	35.6
Case 2	1050	37
Case 3	625	36

respectively, experimental pattern also shown in Table 4. The experimentation with FLC and ANFIS algorithm collected detailed result tabulated in Table 5.

During test period the highest irradiation 1050 W/m² at cell temperature 35°C (case 2) analyzed both

algorithm by (model: UNI-T) four channels DSO and take the voltage waveform with their harmonic spectrum. The (peak to peak) rms value of output voltage is found as 70.76 and 72.14 Volts, respectively. Figure 14 shows the voltage and harmonic spectrum and the corresponding THDs which are found to be 12.3 and 10.3%, respectively. Hence, in different operation modes, ANFIS algorithm improves the voltage quality, power extraction, harmonics elimination as compared to the FLC algorithm.

Table 5: Experimental result

MPPT	Pattern	Converter		Inverter		Efficiency
		Voltage (V_{dc})	Power (P_{dc})	Stepped voltage (V_{ac})	Power (P_{rms})	
FLC	Case 1	12.80	45.58	20.28	28.20	96.61
	Case 2	46.16	118.28	70.16	69.38	97.75
	Case 3	22.13	84.52	42.26	49.21	96.72
ANFIS	Case 1	13.98	48.62	21.34	30.28	97.78
	Case 2	49.25	136.89	72.14	72.42	98.86
	Case 3	24.25	92.78	44.24	52.48	98.15



Fig. 13: Experimental arrangement CHBI (nine levels)

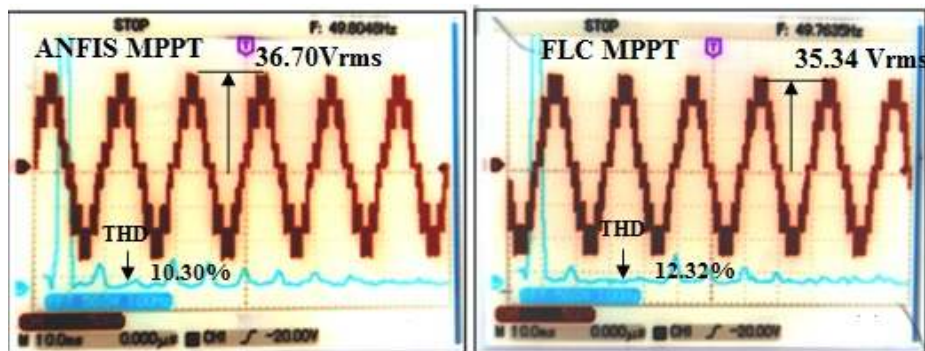


Fig. 14: Experimental result MPPTS output voltage and harmonic spectrum

CONCLUSION

This study analyzes the simulation and experimental performance of FLC and ANFIS MPPT algorithms by stand-alone PV system. The configuration for the proposed system is designed and simulated using MATLAB/SIMULINK and implemented in 16F877A micro controlled prototype. The ANFIS MPPT algorithm improves the voltage quality, power extraction, harmonics elimination as compared to the FLC MPPT controller. The results obtained from ANFIS MPPT algorithm can gain importance in high performance applications such as PV standalone generation system.

REFERENCES

Alajmi, B.N., K.H. Ahmed, S.J. Finney and B.W. Williams, 2011. Fuzzy logic control approach of a modified hill climbing method for maximum power point in microgrid standalone photovoltaic system. *IEEE T. Power Electr.*, 26: 1022-1030.

Ben Salah, C. and M. Ouali, 2011. Comparison of fuzzy logic and neural network in maximum power point tracker for PV systems. *Electr. Pow. Syst. Res.*, 81: 43-50.

Beser, E., B. Arifoglu, S. Camur and E.K. Beser, 2010. A grid-connected photovoltaic power conversion system with single-phase multilevel inverter. *Sol. Energy*, 84: 2056-2067.

Esrarn, T. and P.L. Chapman, 2007. Comparison of photovoltaic array maximum power point tracking techniques. *IEEE T. Energy Conver.*, 22(2): 439-449.

Gao, X., S. Li and R. Gong, 2013. Maximum power point tracking control strategies with variable weather parameters for photovoltaic generation systems. *Sol. Energy*, 93(5): 357-367.

Hohm, D.P. and M.E. Ropp, 2000. Comparative study of maximum power point tracking algorithms using an experimental, programmable, maximum power point tracking test bed. *Proceeding of 28th IEEE Photovoltaic Specialist Conference*, pp: 1699-1702.

- Jung, D.Y., Y.H. Ji, S.H. Park, Y.C. Jung and C.Y. Won, 2011. Interleaved soft-switching boost inverter for photovoltaic power-generation system. *IEEE T. Power Electr.*, 26: 1137-1145.
- Kottas, T.L., Y.S. Boutalis and A.D. Karlis, 2006. New maximum power point tracker for PV arrays using fuzzy controller in close cooperation with fuzzy cognitive Networks. *IEEE T. Energy Conver.*, 21: 793-803.
- Leon, J.I., S. Vazquez, A.J. Watson, G. Franquelo, P.W. Wheeler and J.M. Carrasco, 2013. Feed forward space vector modulation for inverter-phase multilevel cascaded inverters with any DC voltage ratio. *IEEE T. Ind. Electron.*, 56: 315-325.
- Mellit, A. and S.A. Kalogeria, 2011. ANFIS-based modeling for photovoltaic power supply system. *Renew. Energ.*, 36: 250-255.
- Putri, R.I. and M. Rifa, 2012. Maximum power point tracking control for photovoltaic system using neural fuzzy. *Int. J. Comput. Electr. Eng.*, 4: 75-81.
- Ravi, A., P.S. Manoharan and J.V. Anand, 2011. Modeling and simulation of three phase multilevel inverter for grid connected photovoltaic systems. *Sol. Energy*, 85(11): 2811-2819.
- Safari, A. and S. Michele, 2011. Simulation and hardware implementation of incremental conductance MPPT with direct control method using cuk inverter. *IEEE T. Ind. Electron.*, 58(4): 1154-1161.
- Salhi, M. and R. El-Bachtri, 2011. Maximum power point tracker using fuzzy control for photovoltaic system. *Int. J. Res. Rev. Electr. Comput. Eng.*, 1: 2046-2051.
- Tsang, K.M. and W.L. Chan, 2013. Three-level grid-connected photovoltaic inverter with maximum power point tracking. *Energ. Convers. Manage.*, 65: 221-227.